Regenerative Engineering and Translational Medicine
https://doi.org/10.1007/s40883-019-00135-0

Determinants of Hemodialysis Performance:Modeling Fluid and Solute Transport in Hollow-Fiber Dialyzers

Jian Yu[1] · Vipul C. Chitalia[2,3] · Olukemi O. Akintewe[1,4] · Aurelie Edwards[1] · Joyce Y. Wong[1]

Received: 24 June 2019 / Revised: 24 September 2019 / Accepted: 10 October 2019

Abstract

Hemodialysis constitutes the lifeline of patients with end stage renal disease, yet the parameters that affect hemodialyzer performance remain incompletely understood. We developed a computational model of mass transfer and solute transport in a hollow-fiber dialyzer to gain greater insight into the determinant factors. The model predicts fluid velocity, pressure, and solute concentration profiles for given geometric characteristics, membrane transport properties, and inlet conditions. We examined the impact of transport and structural parameters on uremic solute clearance by varying parameter values within the constraints of standard clinical practice. The model was validated by comparison with published experimental data. Our results suggest solute clearance can be significantly altered by changes in blood and dialysate flow rates, fiber radius and length, and net ultrafiltration rate. Our model further suggests that the main determinant of the clearance of unreactive solutes is their diffusive permeability. The clearance of protein-bound toxins is also strongly determined by blood hematocrit and plasma protein concentrations. Results from this model may serve to optimize hemodialyzer operating conditions in clinical practice to achieve better clearance of pathogenic uremic solutes.

Lay Summary

There are nearly 500,000 patients in the USA on kidney dialysis, and a large percentage of these patients use hollow-fiber dialyzers; yet, there is much room for improvement of their performance. To address this issue, we developed a computational model to understand the transport properties of hollow-fiber dialyzers and their effects on clearance of toxins. This study is inspired by the early work of Robert S. Langer in the area of immobilized heparinase in extracorporeal devices, and we continue to look to him as an inspiration for translational research to—in his words—"make a positive impact to improve the quality of life".

Keywords Hemodialysis · Computational Modeling · Solute transport · Uremic Toxins · Albumin binding

Introduction

Hemodialysis (HD) through hollow-fiber dialyzers constitutes the mainstay of renal replacement therapy for patients with end stage renal disease (ESRD). Patients with ESRD are on rise. According to the US Renal Data System (USRDS) Annual Data Report, in 2015 nearly 500,000 patients in the USA were receiving dialysis treatment and 87.3% of newly

Aurelie Edwards and Joyce Y. Wong contributed equally to the work.

✉ Joyce Y. Wong
jywong@bu.edu

Jian Yu
yj1990@bu.edu

Vipul C. Chitalia
vichital@bu.edu

Olukemi O. Akintewe
olukemi@usf.edu

Aurelie Edwards
aued@bu.edu

[1] Department of Biomedical Engineering, Boston University, 44 Cummington Mall, Boston, MA 02215, USA

[2] Renal Section and Cardiovascular Institute, Department of Medicine Boston University School of Medicine, 650 Albany Street, Boston, MA 02118, USA

[3] VA Boston Healthcare System, Boston, MA, USA

[4] Department of Medical Engineering, University of South Florida, Tampa, FL 33620, USA

Published online: 25 November 2019

diagnosed patients began renal replacement therapy with HD [1]. Chronic kidney disease is characterized by the retention of several metabolites, which are referred to as uremic solute/toxins. Uremic toxins are grouped according to their molecular weight and ability to bind to albumin in blood [2, 3]. Among all uremic solutes, protein-bound uremic toxins such as indoxyl sulfate (IS) and p-cresyl glucuronide (pCG) are particularly pathogenic [3, 4]. Emerging evidence has uncovered their vasculotoxic and prothrombotic properties [5–8].

The fundamental rationale of dialysis is to clear blood of retained uremic toxins. The clearance of urea is used clinically to evaluate the effectiveness of dialysis since urea concentrations can be easily determined. Even though urea serves as a surrogate for other uremic solutes, HD does not uniformly remove all types of uremic toxins. The clearance of higher molecular-weight uremic toxins or protein-bound solutes, such as IS, is particularly low with HD [3, 9, 10]. In clinical practice, the composition of dialysate solutions, duration of dialysis, and blood and dialysate flow rates are adjusted within a pre-specified range according to the patient's laboratory results and clinical goals. A better understanding of transport mechanisms and rate-limiting factors may help to build improved hollow-fiber dialyzers and enhance the clinical benefits of HD.

While factors influencing solute clearance during HD can be investigated through bench-top experiments, computational modeling can provide additional insights. Over the last decades, several mathematical models have been developed to simulate counter-current flow within dialyzers, so as to understand the hydrodynamics in hollow-fiber systems. The one-dimensional theory of solute transport in hemodialyzers was described by Jaffrin and colleagues [11] and subsequently applied in many studies [12, 13]. More recent studies have used the full Navier-Stokes equation to compute luminal flow [14], and the Kedem-Katchalsky equation [15] to describe transmembrane flow [16–19]. Each of these models makes particular assumptions, such as neglecting the non-Newtonian behavior of blood, or assuming uniform rates of filtration across the fiber membrane.

In this study, a new two-dimensional axisymmetric computational model was developed to simulate fluid and solute transport in hollow fibers. It differs from previous modeling approaches in that it simultaneously considers (a) both mass transfer and solute transport in a dialyzer, (b) the effect of oncotic pressure in plasma on fluid flow, (c) the impact of hematocrit on blood viscosity, and (d) binding of uremic toxins to plasma proteins. We performed simulations to examine the effects of clinically relevant operating conditions and intrinsic membrane parameters on solute concentration profiles and markers of dialyzer performance such as urea clearance. A detailed understanding of these parameters' impact will help to increase the efficiency of HD.

Methods

Model Description Hollow-fiber dialyzers consist of thousands of cylindrical fibers separating blood from the dialyzing fluid, while maximizing the surface area for fluid and solute exchange. The fiber membranes allow the passage of water and small solutes, but not of red blood cells (RBC) and macromolecules such as albumin. Fluid flow is driven by pressure gradients, and in turn determines solute transfer rates.

We developed a computational model that represents the counter-current flow of blood and dialysate fluid on either side of a hollow-fiber membrane, convection and diffusion of solute within each compartment, and transmembrane flow across the fiber membrane. This steady-state model assumes radial symmetry, and considers one representative hollow fiber (Fig. 1), inside of which blood circulates. Based on the Krogh cylinder approach, the dialysate fluid is taken to flow in the annulus around the fiber and the lateral flux is zero at the outer boundary of the Krogh cylinder. R_f and R_K respectively denote the fiber's inner radius and the Krogh cylinder's outer radius, and N_f is the number of fibers.

Mass Transfer Equations Steady-state fluid velocity and pressure profiles in blood and the dialysate fluid are obtained by solving the Navier-Stokes and continuity equations:

$$\rho(u\cdot\nabla)u = \nabla\cdot\left[-pI + \mu\left(\nabla u + (\nabla u)^T\right)\right]$$
$$\rho\nabla\cdot(u) = 0 \quad (1)$$

where u denotes the velocity vector, p is the pressure, and ρ is the fluid density. We assume a fully developed Poiseuille flow at the inlet of the blood compartment and uniform flow at the inlet of the dialysate compartment. A no-slip condition is applied on the inner and outer surfaces of the filtration membrane. At the inner surface of the fiber membrane, the axial (u_z) and radial (u_r) velocity components satisfy:

$$u_z = 0 \text{ and } u_r = J_v \quad (2)$$

where J_v is the transmembrane fluid flux. At the dialysate compartment outlet, the pressure is zero; at the blood compartment outlet, it is adjusted in every simulation to obtain zero net ultrafiltration, i.e., no net transfer of fluid between blood and dialysate.

Solute Transport Solute transport is driven by diffusion and convection. At steady state, the concentration C_S of solute S in whole blood and the dialysate fluid obeys the following conservation equation:

$$\nabla\cdot(-D_S\nabla C_S) + u\cdot\nabla C_S = R_S \quad (3)$$

where D_S is the diffusion coefficient of solute and R_S is the net reaction rate (set to zero for non-reactive solutes). In blood,

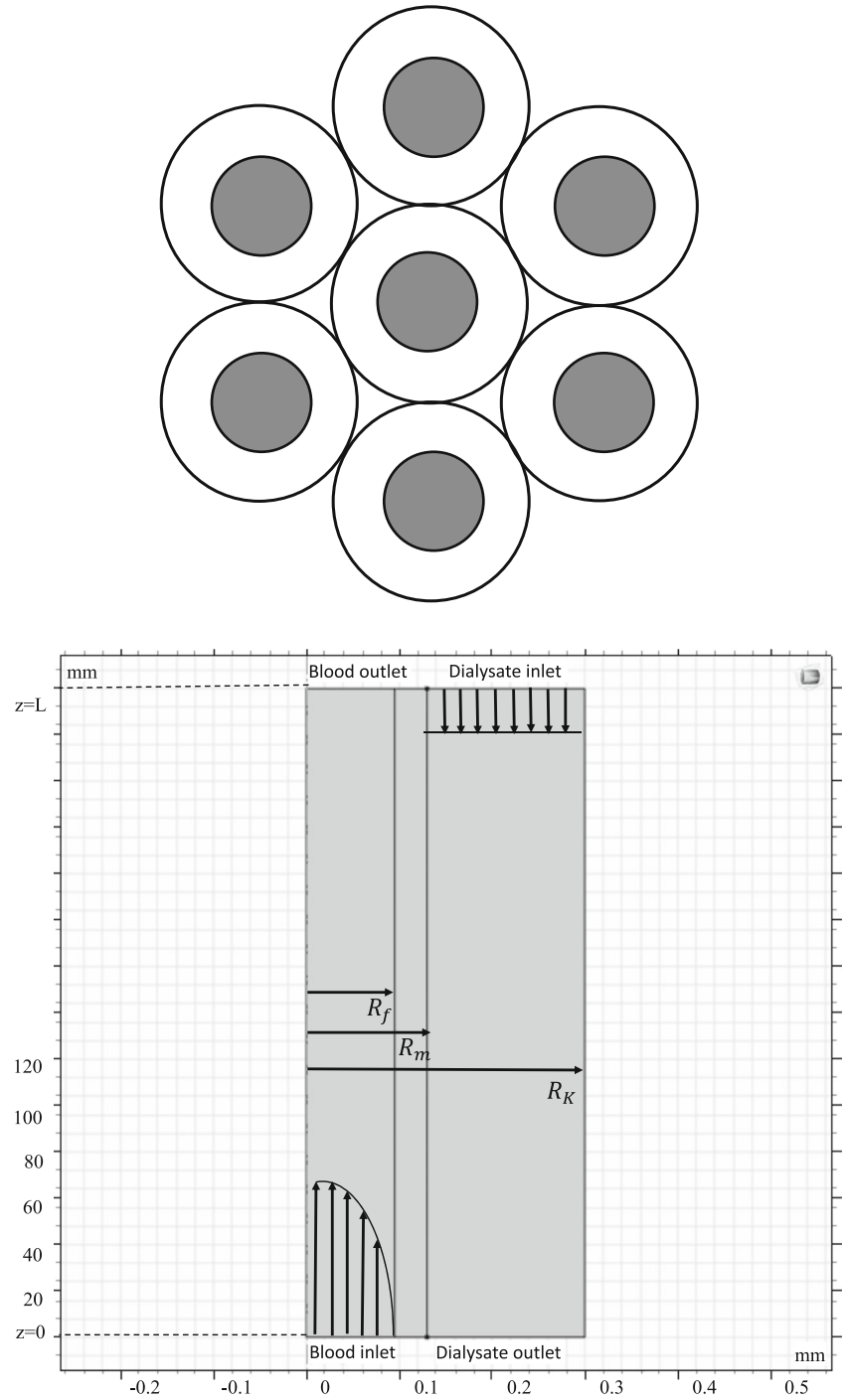

Fig. 1 Schematic representation of model geometry, in cross-sectional (top) and longitudinal (bottom) planes. The grey inner cylinders represent the hollow fibers. The annuli between the outer and inner cylinders represent the spaces in which the dialysate fluid flows, based upon the Krogh cylinder approximation

some uremic toxins (T) bind to plasma proteins to form a protein-toxin complex. In this study, we considered indoxyl sulfate (IS) and p-cresyl glucuronide (pCG), which are respectively characterized by high and low fractions of binding, predominantly to albumin [20]. Assuming that binding can be described as a first-order reversible reaction, the net formation rate of T is given by $R_T = -(k_1 C_A C_T - k_2 C_{AT})$, where C_T is the blood concentration of free uremic toxin, C_{AT} that of bound uremic toxin, C_A that of unbound albumin, and k_1 and k_2 are the association and dissociation rate constants. The values of k_1 and k_2 are estimated based on the binding coefficient, that is, the number of bound toxin molecules per albumin molecule. Albumin has one binding site for pCG [21], and two (a high-affinity and a low-

affinity) binding sites for IS [20]. Note that the binding of pCG does not interfere with that of IS and vice-versa [21].

Concentrations are prescribed at the inlet blood and dialysate compartments. For reactive solutes, the fraction of bound toxins in the infused blood is also specified.

Transmembrane Flow The Kedem-Katchalsky [15] and Patlak [22] equations are used to relate the transmembrane fluid (J_v) and solute (J_S) fluxes to pressure and concentration differences across the fiber membrane:

$$J_v = L_p(\Delta p - \Delta\Pi) = L_p(p_b - p_d - \Pi_b + \Pi_d)$$

$$J_S = J_v(1-\sigma_S)\left(\frac{C_S^b - C_S^d \exp(-P_e)}{1-\exp(-P_e)}\right)$$

$$P_e = \frac{J_v(1-\sigma_S)}{P_S} \tag{4}$$

Fluid flow is driven by the difference in hydrostatic (p) and osmotic (Π) pressures across the membrane: p_b and p_d respectively denote the hydrostatic pressure at the blood/membrane and membrane/dialysate interfaces, and Π_b and Π_d respectively denote the osmotic pressure at these two interfaces. L_p is the hydraulic permeability of the membrane.

In the solute flux equation, the Péclet number (P_e) characterizes the importance of convection relative to diffusion; σ_S is the reflection coefficient of the membrane to solute S; and P_S is the permeability of the membrane to S. The concentrations of S at the blood/membrane and membrane/dialysate interfaces are respectively denoted by C_S^b and C_S^d. Studies have shown that for most electrolytes and small molecular-weight solutes such as urea and creatinine, σ_S can be taken as zero [23].

Mass Balance of Impermeant Species Plasma proteins and RBC do not permeate across the dialyzer membrane. Since the fractional volume of RBC significantly affects the viscosity of blood, we compute the radially-averaged hematocrit ($H(z)$) at each point along the z-axis based on conservation of RBC flow. Similarly, the radially-averaged plasma protein concentration $\left(C_P^{pl}(z)\right)$, which determines the oncotic pressure in blood, is computed based on conservation of plasma protein flow. Blood flow rate varies along the z-axis as:

$$Q_b(z) = Q_{bi} - \int_0^z 2\pi R_f N_f J_v dz \tag{5}$$

We assume that the contribution of small solutes to the osmotic pressure difference across the membrane is negligible relative to that of plasma proteins. The latter are only present on the blood side, thus $\Delta\Pi = \Pi_b$. The local oncotic pressure ($\Pi_b(z)$) is calculated using the empirical equation of Landis and Pappenheimer [24]:

$$\Pi_b(z) = 2.1C_P^{pl} + 0.16\left(C_P^{pl}\right)^2 + 0.009\left(C_P^{pl}\right)^3 \tag{6}$$

where $\left(C_P^{pl}\right)$ is expressed in g/dl and Π_b in mmHg. Plasma concentrations are converted to whole blood concentrations using the hematocrit. The albumin-to-total protein concentration ratio is set to 0.6 [25].

To account for the non-Newtonian behavior of blood, its viscosity (μ_b) is computed based on those of plasma (μ_p) and water (μ_w):

$$\mu_b(z) = \mu_p(z)\cdot(1 + 2.5H(z))$$

$$\mu_p(z) = \mu_w^0 + \left(\mu_p^0 - \mu_w^0\right)\cdot\frac{C_P^{pl}(z)}{C_P^0} \tag{7}$$

The reference values at 37°C are $C_P^o = 7$ g/dl, $\mu_p^o = 1.22$ mPa · s and $\mu_w^o = 0.6915$ mPa · s, respectively [26, 27].

Solute Diffusion Coefficient and Permeability In the absence of specific data, the diffusion coefficient D_S of solute S in blood and dialysate fluid is taken to be a function of its molecular weight MW_S [28]:

$$D_S = 1.62\times10^{-4}\cdot(\mathrm{MW_s})^{-0.552} \tag{8}$$

where D_S is expressed in cm^2/s and MW_s in g/mol. The resulting estimate for creatinine (1.19×10^{-5} cm^2/s) is very close to the experimental value in Ref [29] (1.29×10^{-5} cm^2/s). The permeability of the dialyzer membrane to urea (P_{urea}) and creatinine ($P_{creatinine}$) are respectively taken as 9.76×10^{-6} m/s and 6×10^{-6} m/s [30]. In the absence of data, the permeability to IS and pCG is determined assuming a permeability-to-diffusivity ratio of 5×10^3, as for urea and creatinine. Model parameter values are summarized in Table 1.

Numerical Methods The model described above was programmed under version 5.3 of COMSOL multiphysics®. The default physical modules "Laminar Flow (spf)", "Transport of Diluted Species (tds)", "Coefficient Form Boundary PDE (cb)" and "Chemistry" were used to integrate the equations given the boundary conditions listed above. Both domains were discretized with a mesh of > 500,000 triangle elements.

Model Validation The model was validated by comparing the calculated clearance of specific solutes with published experimental values. The clearance (Cl_S) of solute S is defined as the volume of blood that is completely cleared of S per unit time:

Table 1 Model parameters and initial conditions

Parameters	Description	Value	Units	Reference
R_f	Inner fiber radius	100	μm	[39]
R_m	Radius to outer surface of the membrane	115	μm	[39]
R_K	Radius of the Krogh model	181.8	μm	[39]
L	Fiber length	305	mm	[39]
N_f	Number of fibers	12100	–	[39]
L_p	Hydraulic permeability	1.53×10^{-7}	m/s/mmHg	[30]
D_{urea}	Diffusion coefficient of urea	1.81×10^{-9}	m^2/s	[16]
P_{urea}	Permeability of urea	9.76×10^{-6}	m/s	[30]
$D_{creatinine}$	Diffusion coefficient of creatinine	1.19×10^{-9}	m^2/s	Eq. (8)
$P_{creatinine}$	Permeability of creatinine	6.0×10^{-6}	m/s	[30]
D_{IS}	Diffusion coefficient of IS	8.39×10^{-10}	m^2/s	Eq. (8)
P_{IS}	Permeability of IS	4.2×10^{-6}	m/s	Estimated
D_{pCG}	Diffusion coefficient of pCG	7.16×10^{-10}	m^2/s	Eq. (8)
P_{pCG}	Permeability of pCG	3.6×10^{-6}	m/s	Estimated
k_1	Association rate constant of IS Association rate constant of pCG	$3.6 \times 10^{+7}$ $1.9 \times 10^{+6}$	M/min M/min	[42]
k_2	Dissociation rate constant of IS Dissociation rate constant of pCG	25.50 23.20	s^{-1} s^{-1}	[20] [21]
Q_{bi}	Inlet blood flow	300	ml/min	[17]
Q_{di}	Inlet dialysate flow	500	ml/min	[17]
$H_b(0)$	Inlet hematocrit	25%	–	
$c_p^{pl}(0)$	Inlet plasma protein concentration	7 1.05	g/dl mmol/l	[25]
$c_{Alb}^{pl}(0)$	Inlet plasma albumin concentration	4.2 0.63	g/dl mmol/l	[25]
c_{urea}^{bi}	Inlet blood urea concentration	70 11.7	mg/dl mmol/l	[48]
c_{Cr}^{bi}	Inlet blood creatinine concentration	5 0.442	mg/dl mmol/l	[49]
c_{IS}^{bi}	Inlet blood IS concentration	15.1 0.0708	mg/dl mmol/l	[33]
c_{pCG}^{bi}	Inlet blood pCG concentration	3.5 0.0123	mg/dl mmol/l	[33]

Geometric parameter values are representative of the Baxter CT 190G dialyzer (Baxter Healthcare Co., McGaw Park, IL, USA)

$$Cl_S = \frac{Q_{bi} \times C_S^{bi} - Q_{bo} \times C_S^{bo}}{C_S^{bi}} \quad (9)$$

where Q_{bi} and C_S^{bi} denote blood flow and concentration of S at the inlet, and Q_{bo} and C_S^{bo} denote the corresponding values at the outlet. In healthy persons, blood urea clearance varies between 22 and 64 ml/min, whereas for patients who need HD several times per week, blood urea clearance must increase to 200 or 300 ml/min [31–33]. The native kidney clearance of IS (~ 60 ml/min) is higher than its dialysis clearance (~ 30 ml/min) [31–34], due to its secretion from renal tubular cells via organic anion transporters, which does not occur in HD. The dialysis clearance of pCG is ~ 130 ml/min [35], which is also about 2-fold lower than the native kidney clearance [36].

Results

Base Case

Operating conditions for the base case are given in Table 1. Base-case profiles for pressure, velocities and concentrations indicate that near the blood compartment inlet, the direction of fluid flux is from blood to dialysate; as a result, plasma proteins become increasingly concentrated, which in turn raises the oncotic pressure and lowers the driving force (given by $p_b - p_d - \Pi_b$). At about 1/4th of the fiber length, the transmembrane pressure gradient changes sign, and fluid starts flowing in the opposite direction, from dialysate to blood. The oncotic pressure is predicted to vary between 25 and 55 mmHg, within the experimental range [37, 38]. Urea is transported from blood to dialysate throughout the exchanger; its concentration in the dialysate fluid increases from zero at the entrance to about 83% of the initial urea concentration in blood (results not shown).

Impact of Blood and Dialysate Flow Rates on Clearance

We first examined the dependence of clearance on inlet blood (Q_{bi}) and dialysate (Q_{di}) flows. As shown in Fig. 2a, solute clearance is predicted to increase steeply with increasing Q_{bi}, at a given Q_{di}. This is expected, since clearance is directly proportional to Q_{bi}. When Q_{bi} < 200 ml/min, blood flow is the limiting factor and the slope is close to one. When Q_{bi} reaches 200 ml/min, the rate of solute transport across the fiber membrane becomes more limiting, and the slope diminishes slightly. Raising dialysate flow (i.e., increasing Q_{di} at a given Q_{bi}) also increases the rate of solute removal, but to a lower extent. As shown in Fig. 2b, the dependence of solute clearance on dialysate flow is slightly weaker.

We validated the model by comparing its predictions to experimental (manufacturer) data [39]. Specifically, we compared the calculated and measured clearances of urea and creatinine at 4 different blood flow values (Q_{bi} = 200, 300, 400 and 500 ml/min, with Q_{di} = 500 ml/min). The fractional difference between the computed and experimental values

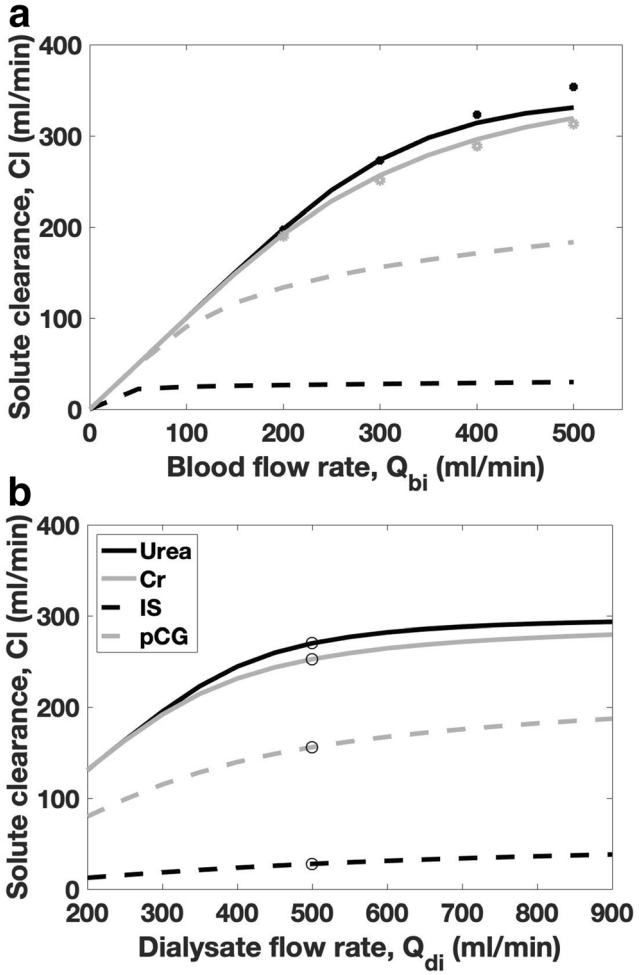

Fig. 2 Clearance of urea (solid black curves), creatinine (solid grey curves), indoxyl sulfate (dashed black curves) and p-cresyl glucuronide (dashed grey curves) as a function of **a** inlet blood flow rate and **b** inlet dialysate flow rate. Dots (panel **a**) represent experimental data from data from Ref. [39] and open circles (panel **b**) indicate base-case values

ranged between 0.26% and 6.5% (Fig. 2a). The predicted clearances of IS and pCG for Q_{bi} = 300 ml/min and Q_{di} = 500 ml/min (namely 27.9 and 155.9 ml/min) are also comparable to published values [31–33, 35].

Impact of Ultrafiltration Rate on Clearance

We then varied the net rate of ultrafiltration (UF) by varying the hydrostatic pressure at the blood compartment outlet (other parameters were kept unchanged). When the outlet pressure is < 25 mmHg, the UF rate is negative, i.e., there is net fluid reabsorption from dialysate into blood. Increasing the outlet pressure raises the net pressure in the blood compartment, thereby enhancing forward filtration and reducing backward filtration, thus increasing net UF. The predicted solute clearance increases almost linearly with the UF rate, because the faster water removal elevates both the transmembrane volume flux and solute concentration in the blood compartment, thereby increasing both solute convection and diffusion across the membrane.

Impact of Blood Composition on Clearance

Patients undergoing hemodialysis often encounter other complications, such as anemia or hypoproteinemia, which can alter the concentration of blood components. We examined the impact of hematocrit (Fig. 3a) and albumin concentration (Fig. 3b) on clearance. Even though these two variables affect oncotic pressures, and therefore fluid filtration, their impact on the clearance of unreactive solutes was negligible over the range of variations considered here.

In contrast, both the hematocrit and plasma albumin concentration are predicted to significantly alter the clearance of IS and pCG; lowering plasma albumin from 4 to 2 g/dl raises the computed clearance of IS and pCG by 100% and 20%, respectively (Fig. 3b). Increasing the hematocrit or decreasing

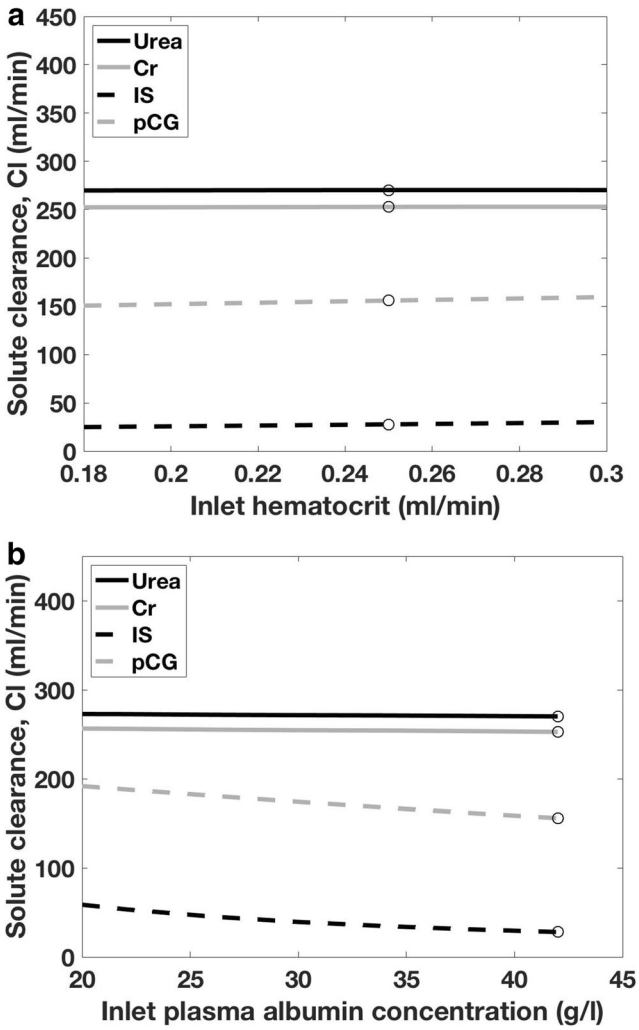

Fig. 3 **a** Solute clearance as a function of the initial inlet hematocrit. **b** Solute clearance as a function of the initial plasma albumin concentration. Open circles indicate base-case values

plasma albumin reduces the whole-blood concentration of albumin and shifts the binding equilibrium to favor dissociation of the albumin-toxin complex. The increased concentration of free toxin in turn augments its clearance during a given dialysis session.

Effects of Dialyzer Geometry on Clearance

Changes in the size of hollow fibers can significant alter fluid flow and therefore dialyzer performance. The model predicts that solute clearance increases with increasing fiber length (L) and decreases with increasing fiber inner radius (R_f). Since the transmembrane velocity ($\sim 10^{-6}$ m/s) is significantly lower than the axial velocity (10^{-2} m/s), the relationship between blood flow and pressure can be approximately described by the Hagen-Poiseuille equation, i.e.: $Q_b = \frac{\pi R_f^4 \Delta p}{8\eta_b L}$. Thus, for a given Q_{bi}, a larger axial pressure drop is obtained with either a longer L or a smaller R_f; achieving zero net ultrafiltration thus entails increasing proximal forward filtration and distal backward filtration (i.e., reabsorption). Since the concentration of uremic toxins is higher in blood than in the dialysate fluid, a greater amount of toxin is then removed, i.e., clearance increases. Note that these predictions agree with experimental data [40, 41].

The model also predicts that solute clearance rises steeply as the outer (Krogh) radius (R_K) is increased from 120 to 200 μm, at which point it reaches its maximum value. Indeed, the volume of the dialysate compartment increases with R_K, thereby diluting solutes therein and enhancing the transmembrane diffusive flux.

Effects of Intrinsic Membrane Parameters on Clearance

Lastly, we investigated the effects of membrane permeability. The hydraulic permeability (L_p) and diffusive permeability (P_S) are intrinsic parameters that depend on membrane thickness, pore size distribution, and fractional pore area. As shown in Fig. 4, the impact of L_p on solute clearance is small if net ultrafiltration is kept equal to zero. In contrast, solute clearance varies significantly with P_S when the latter is varied between 10^{-7} and 10^{-5} m/s. Below 10^{-7} m/s, there is no significant transport across the membrane. Above 10^{-5} m/s, solute clearance reaches a plateau, because the concentration at the outlet approaches zero (results not shown). Overall, these results suggest that the transmembrane solute flux is predominantly driven by diffusion.

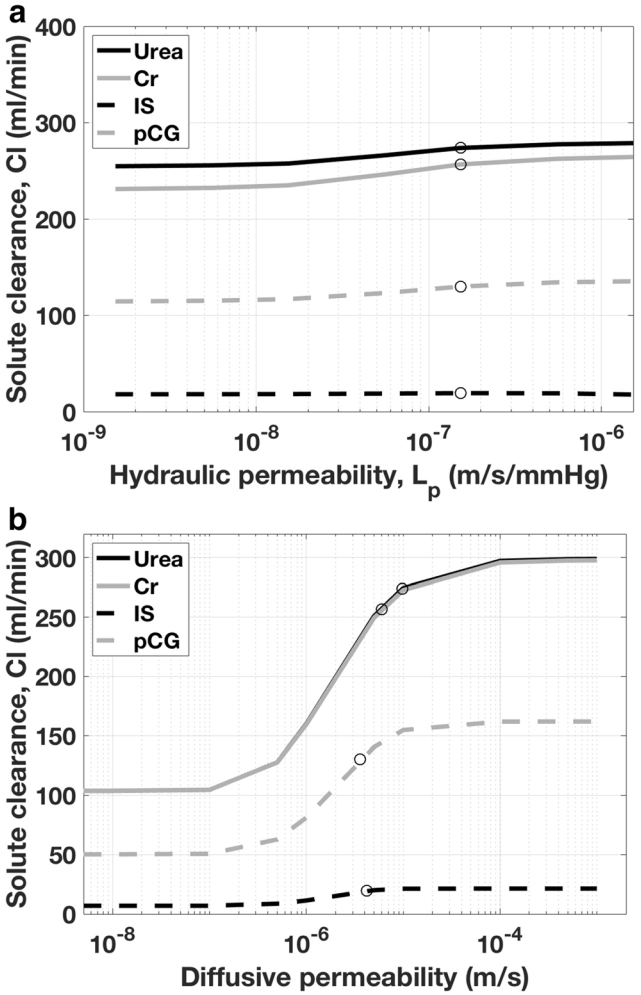

Fig. 4 Solute clearance as a function of **a** hydraulic permeability L_p and **b** solute permeability. Open circles indicate base-case values. Note the log scale on the x-axes

Discussion

The present computational model was developed to investigate the effects of operating conditions, dialyzer geometry and membrane properties on HD performance, as assessed by solute clearance. What distinguishes our model from previous theoretical studies is that (a) it determines fluid and solute transport rates based on the full Navier-Stokes and solute conservation equations while simultaneously accounting for the impact of axially varying oncotic pressure and hematocrit on transmembrane flow, and (b) it applies to both non-reactive and protein-bound solutes. The recent model of Maheshwari et al. also considered the kinetics of protein-bound solutes in a hemodialyzer [42], but it assumed a fixed, linear decrease in plasma flow along the fiber length, and did not take into account back-filtration, the presence of RBC, the effects of oncotic pressure on flow, all of which significantly affect solute clearance. To our knowledge, ours is the first model to examine the impact of plasma albumin and hematocrit on the clearance of protein-bound solutes such as IS and pCG. These two toxins differ in their degree of protein binding: ~ 90% for IS and ~ 10% for pCG [42]. These differences may explain the differential impact of changes in albumin concentration: since a lower fraction of pCG is albumin-bound, its clearance is predicted to be less sensitive to variations in plasma albumin (Fig. 3b).

The model may assist HD prescription in clinical practice and guide the future design of dialyzers. The main findings of this study are recapitulated in Fig. 5. Increasing dialyzer efficiency by raising blood flow or dialysate flow is a common clinical procedure. For in-center standard HD treatment, the KDOQI (Kidney Disease Outcomes Quality Initiative) dialysis guidelines [43] recommend flow rates above 300 ml/min and 500 ml/min for blood and dialysate, respectively. Indeed, our results suggest a steep dependence of urea clearance on blood flow over a large range of values (Fig. 2a). However, increases in blood flow are limited by the fact that a high Q_{bi} may lead to pathophysiological changes such as artery collapse, hypotension, access recirculation [44] and high output heart failure [45]. According to our results, raising Q_{di} from 500 ml/min to 800 ml/min increases urea clearance by 10%, which explains why a Q_{di} value of 800 ml/min is widely adopted in HD. Nonetheless, elevated dialysate flows are not cost-efficient, especially when Q_{di} is > 800 ml/min.

At first glance, it would appear that increasing the rate of ultrafiltration (UF) may help to optimize solute clearance. The model suggests that raising the UF rate from 0 to 20 ml/min increases the clearance of IS and pCG by 4–5%. However, large UF rates may potentially jeopardize the health of patients with tenuous cardiovascular status. Thus, clinical practice guidelines recommend that physicians prescribe the appropriate UF rate for each hemodialysis session [43]. Our results also show that the geometry of dialyzers has a significant impact on their performance. However, from the perspective of manufacturers, the length and radius of hollow fibers cannot be significantly enlarged or shortened owing to technical challenges and cost-efficiency considerations.

The main limitations of our current model are related to geometry, but as described below, they appear to be minimal. To represent mass transfer across one repetitive unit (instead of thousands of fibers), the model uses the Krogh cylinder approach, such that there are empty spaces through which no flow occurs, no matter which alignment of fibers (e.g., hexagonal, square) is chosen (Fig. 1). However, the predicted urea clearance does not depend strongly on the Krogh radius (R_K) once R_K has reached a given threshold, which is close to our base-case R_K value. In addition, the model does not adequately represent the inlet and outlet ports through which fluids flow in/out of the device. Nevertheless, the good agreement between predicted and measured urea and creatinine clearances suggests that the impact of these limitations is modest.

Accurate computational models that closely mimic physiological and pathophysiological conditions could help guide the choice of operating conditions for HD treatment. Developing this model is the initial step in building a platform to study more complex physico-chemical processes in dialyzers, such as the transport of charged species, protein adsorption, and coagulation phenomena, as well as the impact of drug dosage and pharmacokinetics (e.g., following administration of antibiotics) during hemodialysis.

With respect to protein adsorption, the physicochemical properties of the membrane, including chemical composition, porosity, and surface roughness, significantly contribute to membrane adsorption resistance. A recent study found that

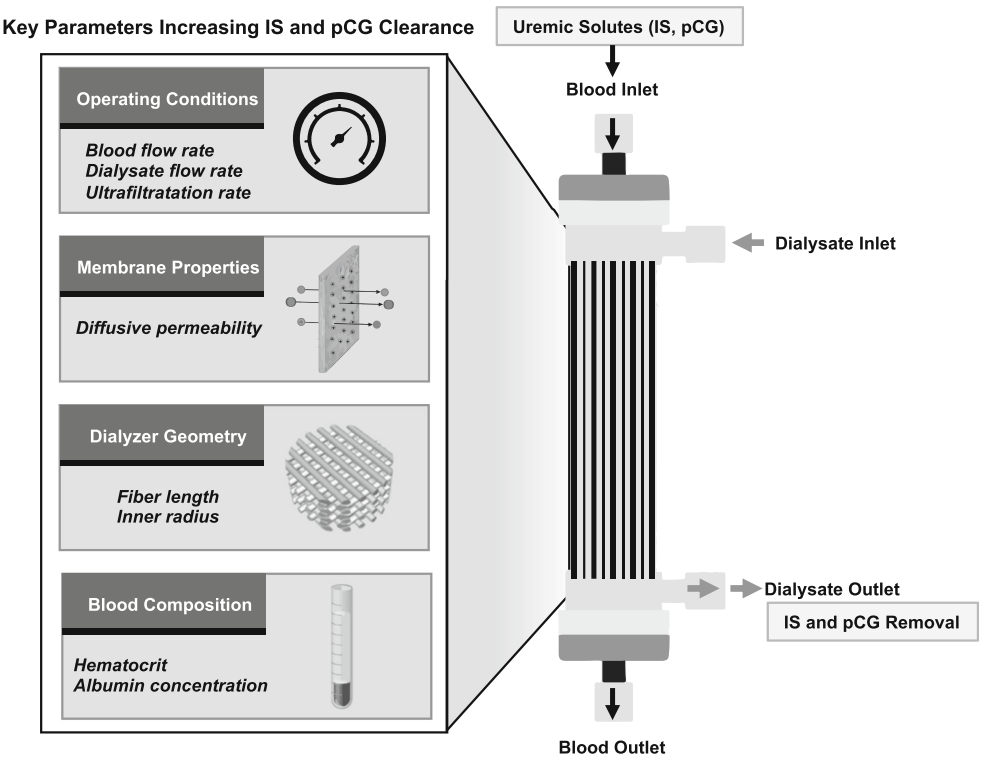

Fig. 5 Schematic representation of the key parameters that impact the clearance of uremic toxins

exposure of polysulfone/polyethersulfone dialyzer membranes to serum proteins had a large impact on solute clearance, whereas exposure of asymmetric cellulose triacetate membranes had minimal effects on transport properties [46]. The Baxter CT 190G hemodialyzer upon which our calculations are based is composed of homogeneous cellulose triacetate membranes, the surface of which is thought to be less smooth than that of asymmetric cellulose triacetate membranes, but we were unable to find published studies comparing protein adsorption between the two membrane types. A recent study used proteomics to investigate protein adsorption properties and found differences between low- and high-flux Polyamix (a blend of polyarylethersulfone, polyvinylpyrrolidone, and polyamide) membranes [47]. We also note that protein adsorption can lead to platelet activation and complement activation, which affect dialyzer membrane performance. In particular, the proteomic studies of Han et al. [47] provide a useful tool to assess the biocompatibility of dialysis membranes, as specific proteins associated with either platelet or complement activation can be identified. As more experimental studies are conducted, quantitative, membrane-specific results can be incorporated in our model. Specifically, future extensions of the model should account for the adsorption of proteins and other molecules, particle aggregation, and surface heterogeneities.

In conclusion, our results suggest that solute clearance can be optimized by increasing not only membrane permeability but also blood flow rate, dialysate flow rate, and net ultrafiltration; increasing the length of the hollow fiber membrane or decreasing its inner radius may also enhance solute removal from blood (Fig. 5). Our model can serve as a useful platform to build upon in order to optimize HD performance.

Acknowledgments We thank Dr. Belghasem in the Department of Pathology and Laboratory Medicine at Boston University for his contribution to the summary figure. We also thank James K. Goebel in the Engineering Information Technology Office at Boston University for his help in setting up the COMSOL Batch mode.

Funding Information This project was funded by National Institutes of Health (NIH) grants R01-HL132325 and R01-CA175382 to VCC, NIH grant T32 HL007224 to OA, and Boston University's College of Engineering Distinguished Professorship support to JYW.

References

1. Saran R, et al. US Renal Data System 2017 Annual Data Report: epidemiology of kidney disease in the United States. Am J Kidney Dis. 2018;**71**(3S1):A7.
2. Vanholder R, Schepers E, Pletinck A, Nagler EV, Glorieux G. *The* uremic toxicity of indoxyl sulfate and p-cresyl sulfate: a systematic review. J Am Soc Nephrol. 2014;**25**(9):1897–907.
3. Liabeuf S, Drueke TB, Massy ZA. Protein-bound uremic toxins: new insight from clinical studies. Toxins (Basel). 2011;**3**(7):911–9.
4. Niwa T. Targeting protein-bound uremic toxins in chronic kidney disease. Expert Opin Ther Targets. 2013;**17**(11):1287–301.
5. Vanholder R, Glorieux G. Introduction: uremic toxicity - state of the art 2014. Semin Nephrol. 2014;**34**(2):85–6.
6. Shashar M, Francis J, Chitalia V. Thrombosis in the uremic milieu–emerging role of "thrombolome". Semin Dial. 2015;**28**(2):198–205.
7. Kolachalama VB, Shashar M, Alousi F, Shivanna S, Rijal K, Belghasem ME, et al. Uremic solute-aryl hydrocarbon receptor-tissue factor axis associates with thrombosis after vascular injury in humans. J Am Soc Nephrol. 2018;**29**(3):1063–72.
8. Shashar M, et al. Targeting STUB1-tissue factor axis normalizes hyperthrombotic uremic phenotype without increasing bleeding risk. Sci Transl Med. 2017:**9**(417).
9. Meyer TW, Walther JL, Pagtalunan ME, Martinez AW, Torkamani A, Fong PD, et al. The clearance of protein-bound solutes by hemofiltration and hemodiafiltration. Kidney Int. 2005;**68**(2):867–77.
10. Meert N, et al. Effective removal of protein-bound uraemic solutes by different convective strategies: a prospective trial. Nephrol Dial Transplant. 2009;**24**(2):562–70.
11. Jaffrin MY, Gupta BB, Malbrancq JM. A one-dimensional model of simultaneous hemodialysis and ultrafiltration with highly permeable membranes. J Biomech Eng. 1981;**103**(4):261–6.
12. Werynski A, Waniewski J. Theoretical description of mass transport in medical membrane devices. Artif Organs. 1995;**19**(5):420–7.
13. Pallone TL, Hyver S, Petersen J. The simulation of continuous arteriovenous hemodialysis with a mathematical model. Kidney International. 1989;**35**(1):125–33.
14. Donato D, et al. Optimization of dialyzer design to maximize solute removal with a two-dimensional transport model. J Membrane Sci. 2017;**541**:519–28.
15. Kedem O, Katchalsky A. Thermodynamic analysis of the permeability of biological membranes to non-electrolytes. Biochimica et Biophysica Acta. 1958;**27**:229–46.
16. Liao Z, Poh CK, Huang Z, Hardy PA, Clark WR, Gao D. A numerical and experimental study of mass transfer in the artificial kidney. J Biomech Eng. 2003;**125**(4):472–80.
17. Lee JC, Lee K, Kim HC. Mathematical analysis for internal filtration of convection-enhanced high-flux hemodialyzer. Comput Methods Programs Biomed. 2012;**108**(1):68–79.
18. Yamamoto K, Matsuda M, Hirano A, Takizawa N, Iwashima S, Yakushiji T, et al. Computational evaluation of dialysis fluid flow in dialyzers with variously designed jackets. Artif Organs. 2009;**33**(6):481–6.
19. Aniort J, Chupin L, Cindea N. Mathematical model of calcium exchange during haemodialysis using a citrate containing dialysate. Math Med Biol. 2018;**35**(suppl_1):87–120.
20. Viaene L, Annaert P, de Loor H, Poesen R, Evenepoel P, Meijers B. Albumin is the main plasma binding protein for indoxyl sulfate and p-cresyl sulfate. Biopharm Drug Dispos. 2013;**34**(3):165–75.
21. Yi D, et al. Determination of the binding properties of p-cresyl glucuronide to human serum albumin. Biochimie. 2018;**150**:1–7.
22. Patlak CS, Goldstein DA, Hoffman JF. The flow of solute and solvent across a two-membrane system. J Theor Biol. 1963;**5**(3):426–42.
23. Annan K. Mathematical modeling for hollow fiber dialyzer: blood and HCO 3 - -dialysate flow characteristics. IJPAM. 2012;**79**:425–52.
24. Landis, E.M. and J.F. Pappenheimer, *Exchange of substances through the capillary walls*, in *Handbook of physiology*. 1963, American Physiological Society: Washington, DC. p. pp. 961-1034.
25. Hall, J.E., Guyton and Hall textbook of medical physiology. 13 ed. 2016, Philadelphia, PA: Elsevier.
26. Pallone TL, Petersen J. A mathematical model of continuous arteriovenous hemofiltration predicts performance. ASAIO Trans. 1987;**33**(3):304–8.

27. Lightfoot EN. Transport phenomena and living systems—biomedical aspects of momentum and mass transport. New York City, NY: Wiley; 1974.
28. Preston, B.N., et al., *Diffusion of dextran at intermediate concentrations.* Journal of the Chemical Society, Faraday Transactions 1: Physical Chemistry in Condensed Phases, 1982. **78**(4): p. 1209-1221.
29. Collins MC, Ramirez WF. Transport through polymeric membranes. J Phys Chem. 1979;**83**(17):2294–301.
30. Liao Z, et al. Measurement of hollow fiber membrane transport properties in hemodialyzers. J Membrane Sci. 2005;**256**(1):176–83.
31. Luo FJ, Patel KP, Marquez IO, Plummer NS, Hostetter TH, Meyer TW. Effect of increasing dialyzer mass transfer area coefficient and dialysate flow on clearance of protein-bound solutes: a pilot cross-over trial. Am J Kidney Dis. 2009;**53**(6):1042–9.
32. Sirich TL, Funk BA, Plummer NS, Hostetter TH, Meyer TW. Prominent accumulation in hemodialysis patients of solutes normally cleared by tubular secretion. J Am Soc Nephrol. 2014;**25**(3):615–22.
33. Eloot S, Schneditz D, Cornelis T, van Biesen W, Glorieux G, Dhondt A, et al. Protein-bound uremic toxin profiling as a tool to optimize hemodialysis. PLOS ONE. 2016;**11**(1):e0147159.
34. Poesen R, et al. The influence of renal transplantation on retained microbial-human co-metabolites. Nephrol Dial Transplant. 2016;**31**(10):1721–9.
35. Etinger A, Kumar SR, Ackley W, Soiefer L, Chun J, Singh P, et al. The effect of isohydric hemodialysis on the binding and removal of uremic retention solutes. PLOS ONE. 2018;**13**(2):e0192770.
36. Poesen R, Evenepoel P, de Loor H, Kuypers D, Augustijns P, Meijers B. Metabolism, protein binding, and renal clearance of microbiota-derived p-cresol in patients with CKD. Clin J Am Soc Nephrol. 2016;**11**(7):1136–44.
37. Schneditz D. TMP revisited: the importance of plasma colloid osmotic pressure in high-flux dialysers. Nephrol Dial Transpl. 2011;**26**(2):411–3.
38. Schneditz D, et al. The influence of colloid osmotic pressure on hydrostatic pressures in high- and low-flux hemodialyzers. Artificial Organs. 2018;**42**(5):525–32.
39. *Baxter, Manufacturer's Specification Sheet of CT190G Dialyzer.* . Available from: https://www.baxter.com/assets/downloads/al09086-cellulosic-brochure-final.pdf.
40. Sato Y, Mineshima M, Ishimori I, Kaneko I, Akiba T, Teraoka S. Effect of hollow fiber length on solute removal and quantification of internal filtration rate by Doppler ultrasound. Int J Artif Organs. 2003;**26**(2):129–34.
41. Ronco C, Brendolan A, Lupi A, Metry G, Levin NW. Effects of a reduced inner diameter of hollow fibers in hemodialyzers. Kidney Int. 2000;**58**(2):809–17.
42. Maheshwari V, Thijssen S, Tao X, Fuertinger D, Kappel F, Kotanko P. A novel mathematical model of protein-bound uremic toxin kinetics during hemodialysis. Sci Rep. 2017;**7**(1):10371.
43. National Kidney Foundation. KDOQI Clinical Practice Guideline for Hemodialysis Adequacy. *update*. Am J Kidney Dis, 2015. *2015*;**66**(5):884–930.
44. Besarab A, Sherman R. The relationship of recirculation to access blood flow. Am J Kidney Dis. 1997;**29**(2):223–9.
45. Al-Ghonaim M, et al. Relation between access blood flow and mortality in chronic hemodialysis patients. Clin J Am Soc Nephrol. 2008;**3**(2):387–91.
46. Kim TR, Hadidi M, Motevalian SP, Sunohara T, Zydney AL. Effects of plasma proteins on the transport and surface characteristics of polysulfone/polyethersulfone and asymmetric cellulose triacetate high flux dialyzers. Artificial Organs. 2018;**42**(11):1070–7.
47. Han, S., et al., *Proteomics investigations into serum proteins adsorbed by high-flux and low-flux dialysis membranes.* PROTEOMICS â€“ Clinical Applications, 2017. **11**(11-12): p. 1700079.
48. Castro MC, Romao JE Jr, Marcondes M. Measurement of blood urea concentration during haemodialysis is not an accurate method to determine equilibrated post-dialysis urea concentration. Nephrol Dial Transplant. 2001;**16**(9):1814–7.
49. Nisha R, et al. Biochemical evaluation of creatinine and urea in patients with renal failure undergoing hemodialysis. J Clin Path Lab Med. 2017;**1**:1–5.